Nucleation and Growth of Islands on GaAs Surfaces

A. R. Avery, H. T. Dobbs, D. M. Holmes, B. A. Joyce, and D. D. Vvedensky
Interdisciplinary Research Centre for Semiconductor Materials, Imperial College, London SW7 2BZ, United Kingdom
(Received 20 June 1997)

Submonolayer island-size distributions are obtained with scanning tunneling microscopy and used to infer the nucleation and growth kinetics of islands on the three low-index surfaces of GaAs. Comparison with Monte Carlo simulations reveals that on the (110) and (111)*A* surfaces, random nucleation is followed by the attachment and detachment of single atoms at island edges. But on the (001) surface (using As_4), nucleation is initiated in the trenches of the 2×4 reconstruction by pairs of Ga atoms. Growth then proceeds over locally filled trenches, also by the capture of pairs of Ga atoms. [S0031-9007(97)04533-X]

PACS numbers: 68.35.Bs, 61.16.Ch, 81.15.Hi

The nucleation and growth of two-dimensional islands on semiconductor surfaces is fundamental to the fabrication of all quantum heterostructures. The basic atomistic processes that drive island kinetics are adatom mobility, adatom interactions during island formation, and interactions between adatoms and step edges that are responsible for island growth. A detailed understanding of how these processes are affected by growth conditions, surface orientations, and surface reconstructions is therefore essential for utilizing epitaxial growth to its full capability.

The basic tenets of island nucleation and growth have been known for some time [1], but the advent of the scanning tunneling microscope (STM) has led to a resurgence in the study of island kinetics by allowing as-grown surface morphologies to be imaged in real space. This has spawned a huge effort aimed at characterizing submonolayer epitaxial growth prior to significant coalescence, where island statistics can be used to infer certain aspects of their nucleation and growth kinetics. Perhaps the most far-reaching result of this work [2] is that the density n_s of s-atom islands can be written as

$$n_s = \frac{\theta}{\langle s \rangle^2} f(s/\langle s \rangle), \tag{1}$$

where $\langle s \rangle$ is the average island size, θ is the coverage, and f is a scaling function. STM measurements [3] are consistent with (1) and, together with theoretical studies, have shown how f is affected by mechanisms such as adatom attachment and detachment [4,5], magic island sizes [6], adatom exchange [7,8], and the mobility of small adatom clusters [9–11].

In this Letter we report an STM study of submonolayer islands in the precoalescence regime grown by molecular-beam epitaxy (MBE) on the three low-index surfaces of GaAs. Monte Carlo simulations are used to confirm the atomistic mechanisms of island kinetics inferred from the STM images. For the growth conditions used, islands on the (110) and (111)*A* surfaces are found to form by the binding of two or more Ga adatoms, with subsequent growth occurring by the net attachment of single Ga adatoms to island edges. But growth on GaAs(001)-(2×4) follows an altogether different scenario that cannot be reconciled with any of the mechanisms cited above. Island formation is initiated by *pairs* of Ga atoms in the missing dimer trenches of the 2×4 reconstruction. Growth then proceeds both along trenches and across locally filled trenches, in each case by the addition of *pairs* of Ga atoms. These conclusions are consistent with modulated-beam studies on GaAs(001) [12], which showed a *second-order* reaction between adjacent Ga atoms and As_4, and on GaAs(111)*A* [13], which indicated a *first-order* Ga-As_2 reaction. They are also consistent with simulations of GaAs(001) based on electron counting [14].

The GaAs surfaces were prepared and imaged in a combined ultra-high-vacuum STM (Omicron GmbH, Germany) and MBE (DCA, Finland) system. The singular n^+-doped GaAs substrates were mounted on molybdenum blocks using indium solder without any additional *ex situ* processing. The (001), (110), and (111)*A* substrates were prepared under As-stable conditions on which GaAs buffer layers were grown using standard conditions [15]. Submonolayer films were then grown with the coverage determined from Ga flux measurements using the period of reflection high-energy electron diffraction (RHEED) specular-beam intensity oscillations on (001) substrates. The surfaces were monitored throughout by RHEED, with the (001), (110), and (111)*A* orientations exhibiting characteristic (2×4), (1×1), and (2×2) diffraction patterns, respectively.

The substrates were quenched rapidly to room temperature by transferral (within a few seconds) from the growth chamber directly into the STM chamber, where rapid cooling ensued in the absence of any background arsenic flux. Stable room-temperature STM images were obtained with no noticeable thermal drift within a few minutes of deposition. The experiments were repeated with several samples and tips for each orientation and with a number of coverages and growth conditions. The

 0031-9007/97/79(20)/3938(4)$10.00

images were obtained in constant current mode using sample biases between -1.8 and -2.8 V (filled states) and tunneling currents between 0.1 and 0.25 nA.

STM images of GaAs(001)-(2×4), GaAs(110), and GaAs(111)*A*-(2×2) taken after the deposition of 0.2 monolayers (ML) of Ga are shown in Fig. 1. The growth temperatures were 580 °C for the (001) and 480 °C for the (110) and (111)*A* surfaces, with an atomic As:Ga ratio of 6:1 and a growth rate of 0.08 ML/s for all surfaces. The (001) and (110) surfaces were grown with As_4 and the (111)*A* was grown with As_2.

The islands on the (110) and (111) surfaces exhibit similarities both in density and morphology, but the morphology of the (001) surface is strikingly different from these, showing a much higher density of smaller islands. An analysis of several images, in fact, yields island densities of 17 000, 1700, and 1900 μm^{-2} for the (001), (110), and (111)*A* surfaces, respectively, i.e., *an order of magnitude* difference between the island density on the (001) surface and those on the other two surfaces *at the same nominal coverage*.

Figure 2 shows the island-size distributions obtained from STM images, expressed in the form (1) [16], compared with distributions produced by Monte Carlo simulations. The distributions for the (110) and (111)*A* surfaces are qualitatively similar and have the general form expected for critical island sizes $i^* > 1$ and single adatom capture [2,4,17]. The corresponding simulated distributions are labeled by the ratio λ of the detachment rate of single atoms from island edges to the capture rate of adatoms by all islands [4], with the value for the (111)*A* surface ($\lambda \approx 10$) being discernibly larger than that for the (110) surface ($\lambda \approx 5$). Despite the slight offset near $s/\langle s \rangle \approx 1$ for the (111)*A* surface, the overall level of agreement between the simulated and measured distributions allows us to conclude that for these two surfaces, islands nucleate by the binding of two *or more* Ga adatoms and grow by the net capture of *single* Ga adatoms.

The distribution for GaAs(001)-(2×4) in Fig. 2 suggests that the island kinetics which are appropriate for the (110) and (111)*A* surfaces are not followed by this surface. To understand the reasons for this, we consider the atomic structure of the 2×4 reconstruction. The widely accepted view [18] is that for MBE-grown surfaces the unit cell consists of two As dimers and two missing dimers in the uppermost layer, with the exposed As atoms in the third layer forming dimers [Fig. 3(a)].

A higher resolution image of a GaAs(001)-(2×4) surface is shown in Fig. 4. This surface was grown at 440 °C using As_4 with an atomic As:Ga ratio of 1:1 and a growth rate of 0.05 ML/s. The dark stripes running along the $[\bar{1}10]$ direction correspond to the missing dimer rows [Fig. 3(a)]. Because the Ga trench sites within these rows [the crosses in Fig. 3(a)] are better coordinated, they are more likely to be occupied during initial deposition than top-layer sites [19]. Hence, the interruptions of the

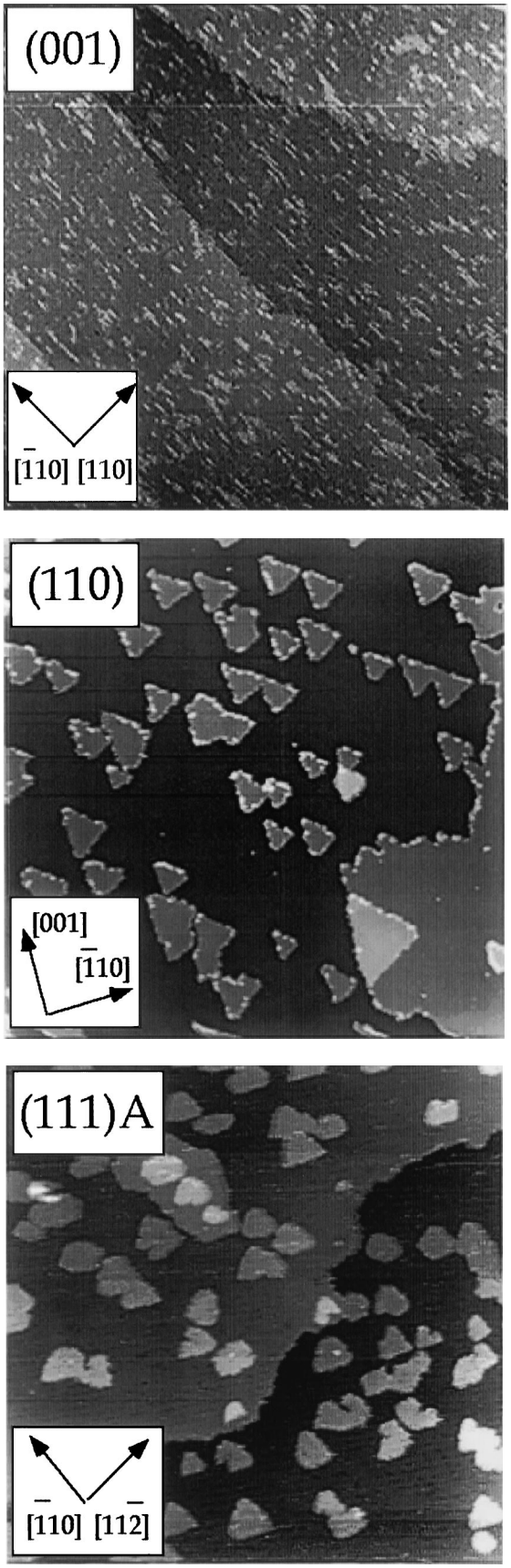

FIG. 1. Filled-state STM images of the low-index GaAs surfaces taken after the deposition of 0.2 ML of Ga. The scan area for each image is 2000 Å $\times$ 2000 Å.

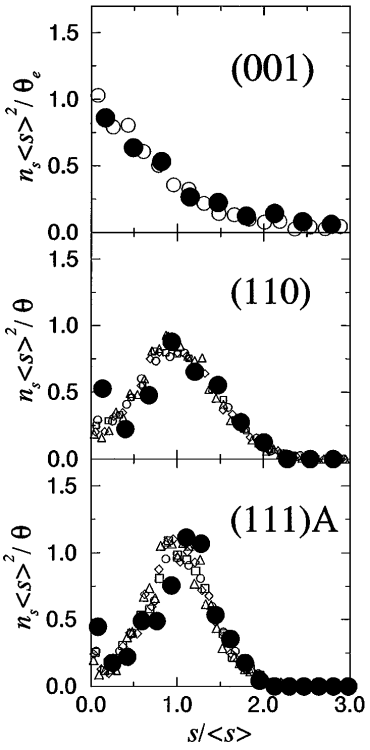

FIG. 2. Island-size distributions obtained from STM images (filled circles) and from simulations (open symbols) at 0.2 ML. The simulations for (001)-(2 × 4) are described in the text; those for (110) and (111)*A*-(2 × 2) are taken from Ref. [4].

dimer rows (the circled region in Fig. 4) correspond to the filled trenches shown in Fig. 3(b). The modulated-beam study in Ref. [12] suggests that this structure forms when two Ga adatoms bind simultaneously to an As_2 produced by the pairwise dissociation of As_4; a second As_2 then saturates the remaining Ga bonds. For growth with an As_2 source, no predissociation would be required. The STM scan along [110] of a feature of the type circled in Fig. 4 supports the structural model in Fig. 3(b). Although trench sites are more favorable for Ga than top-layer sites, trench filling does not occur readily, since chains of more than a few occupied trench sites are rarely seen in the STM images.

The final step of island formation is growth across the trenches. For the reasons noted above, this is also expected to occur by the pairwise attachment of Ga adatoms, producing structures of the type shown in Fig. 3(c). The boxed region in Fig. 4 is such a structure. Close examination of Fig. 4 shows that growth along the [110] direction can only occur when corresponding sites in adjacent trenches are occupied. Thus, growth along both the [110] and [$\bar{1}$10] directions is limited by trench filling.

We have constructed a kinetic Monte Carlo simulation to show that the scenario we propose is consistent with the STM observations. The crystal is modeled as a simple cubic solid-on-solid lattice and atoms interact only with their nearest neighbors. Trenches are constructed by removing every alternate pair of atoms across the lattice. Rows

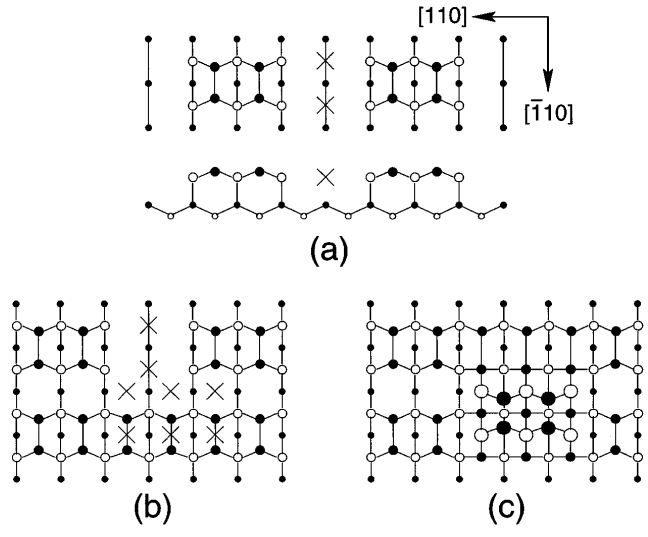

FIG. 3. (a) Side and plan views of GaAs(001)-(2 × 4) prior to deposition, (b) a filled trench, and (c) growth across a filled trench. The crosses in (a) and (b) indicate the Ga sites that produce the structures in (b) and (c), respectively. Ga and As atoms are indicated by unfilled and filled circles, respectively.

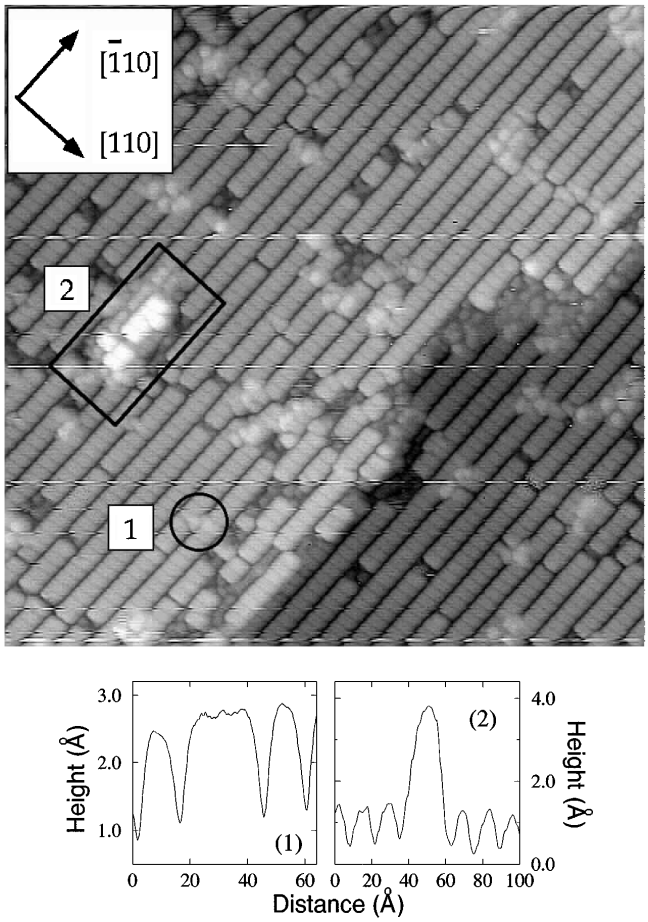

FIG. 4. Filled-state STM image of GaAs(001)-(2 × 4) after the deposition of 0.05 ML of Ga. The scan area is 450 Å × 450 Å. Also shown are line scans along [110] through structures of the type that are circled and boxed.

running parallel to the trenches are grouped into pairs, with the bonding E_p between paired atoms in consecutive rows being stronger than the bonding E_u between unpaired atoms in these rows. This pairing results in islands growing by the pairwise attachment of adatoms and stabilizes the trench structure. The bond E_p is also stronger than the bond E_n between atoms in adjacent rows perpendicular to the trenches, which controls the anisotropy of the islands. Finally, the pairing between adjacent rows switches in alternate layers, so that a pair in layer n sits on top of two pairs in layer $n - 1$. This makes nucleation in the first layer likely only on a section overlapping a locally filled trench. The energy barrier for single atom diffusion is E_s.

The distribution function obtained from this model with the experimental temperature and Ga flux and with the parameters $E_s = 1.3$ eV, $E_p = 0.50$ eV, $E_u = 0.075$ eV, and $E_n = 0.16$ eV is shown in Fig. 2(a). The attempt frequency for all processes was taken to be 3×10^{13} Hz. The agreement with the measured distribution function is seen to be quite satisfactory. The measured and simulated island densities are also in close agreement and the island morphologies (not shown) have the same general features as those shown in Fig. 4. No model with single atom attachment was able to reproduce the measured island distribution, density, and morphology [20].

There are several consequences and extensions that are suggested by our results. First is the effect of the As. By varying the As flux (at fixed Ga flux), the effect of As kinetics on island morphologies and size distributions can be isolated and identified. A related issue is the effect of using As_2 instead of As_4, particularly on the (001) surface. Because As_2 does not require the presence of adjacent Ga atoms to bind to the surface, the kinetics of island nucleation and growth need no longer be dominated by pairwise Ga attachment kinetics. This would affect both island sizes and morphologies and may explain the subtle differences observed between growth with As_2 and As_4 [22].

Then there is the applicability of our results to other III-V systems. Since GaAs growth is determined by the chemistry of As_4, we expect our results to carry over to the homoepitaxial growth of AlAs and InAs. But the effect of changing the group-V species is less clear. The similarities of P and As, both in the formation of gas phase dimers and tetramers and in surface dimerization, suggests that growth from P_4 and As_4 is correspondingly similar, including the pairwise addition of group-III adatoms on (001) surfaces. Similarities may also exist for the antimonides, but there is not enough experimental evidence upon which to base a conclusion.

Finally, we discuss the implications of our work for the heteroepitaxial growth of InAs on GaAs. Although there is a constant lattice mismatch ($\approx 7\%$) on the three low-index orientations, very different growth modes are observed. Stranski-Krastanov growth of coherent three-dimensional islands [23] occurs only on (001); on the other two orientations strain relaxation involves misfit dislocation formation and continuous two-dimensional growth [24]. Figures 1 and 2 are very suggestive, but similar work is needed for InAs/GaAs [25] to address the atomistic mechanisms behind this behavior.

[1] J. A. Venables, G. D. T. Spiller, and M. Hanbücken, Rep. Prog. Phys. **47**, 399 (1984), and references therein.
[2] J. W. Evans and M. C. Bartelt, J. Vac. Sci. Technol. A **12**, 1800 (1994).
[3] J. A. Stroscio and D. T. Pierce, Phys. Rev. B **49**, 8522 (1994); B. Muller, L. Nedelmann, B. Fischer, H. Brune, and K. Kern, Phys. Rev. B **54**, 17 858 (1996).
[4] C. Ratsch, P. Šmilauer, A. Zangwill, and D. D. Vvedensky, Surf. Sci. **329**, L599 (1995).
[5] D. Kandel, Phys. Rev. Lett. **78**, 499 (1997).
[6] M. Schroeder and D. E. Wolf, Phys. Rev. Lett. **74**, 2062 (1995).
[7] D. D. Chambliss and K. E. Johnson, Phys. Rev. B **50**, 5012 (1994).
[8] A. Zangwill and E. Kaxiras, Surf. Sci. **326**, L483 (1995).
[9] M. C. Bartelt, S. Gunther, E. Kopatzki, R. J. Behm, and J. W. Evans, Phys. Rev. B **53**, 4099 (1996).
[10] L. Kuipers and R. E. Palmer, Phys. Rev. B **53**, R7646 (1996).
[11] I. Furman and O. Biham, Phys. Rev. B **55**, 7917 (1997).
[12] C. T. Foxon and B. A. Joyce, Surf. Sci. **50**, 434 (1975).
[13] J. R. Arthur, J. Appl. Phys. **39**, 4032 (1968).
[14] T. Ito and K. Shiraishi, Surf. Sci. **357–358**, 486 (1996).
[15] A. R. Avery, D. M. Holmes, J. L. Sudijono, T. S. Jones, and B. A. Joyce, Surf. Sci. **323**, 91 (1995).
[16] For the (001) surface, the island densities and the coverage θ_e refer to quantities measured on the *topmost* layer of the 2×4 reconstruction.
[17] J. G. Amar and F. Family, Phys. Rev. Lett. **74**, 2066 (1995).
[18] T. Hashizume, Q. K. Zue, J. Zhou, A. Ichimiya, and T. Sakurai, Phys. Rev. Lett. **73**, 2208 (1994); A. R. Avery, C. M. Goringe, D. M. Holmes, J. L. Sudijono, and T. S. Jones, Phys. Rev. Lett. **76**, 3344 (1996); J. E. Northrup and S. Froyen, Phys. Rev. B **50**, 2015 (1994).
[19] A. Kley, P. Ruggerone, and M. Scheffler, Phys. Rev. Lett. (to be published).
[20] Other mechanisms can produce distributions which are indistinguishable from that in Fig. 2(a) (including evaporation [21] and extreme anisotropy), but these are either inoperative for the GaAs(001) surface (evaporation) or produce a morphology inconsistent with that in Fig. 1(a).
[21] P. Jensen, H. Larralde, and A. Pimpinelli, Phys. Rev. B **55**, 2556 (1997).
[22] J. H. Neave, P. K. Larsen, J. F. van der Veen, P. J. Dobson, and B. A. Joyce, Surf. Sci. **133**, 267 (1983).
[23] P. M. Petroff and S. P. DenBaars, Superlattices Microstruct. **15**, 15 (1994).
[24] B. A. Joyce, J. L. Sudijono, J. G. Belk, H. Yamaguchi, X. M. Zhang, H. T. Dobbs, A. Zangwill, D. D. Vvedensky, and T. S. Jones, Jpn. J. Appl. Phys. **36**, 4111 (1997).
[25] V. Bressler-Hill, S. Varma, A. Lorke, B. Z. Nosho, P. M. Petroff, and W. H. Weinberg, Phys. Rev. Lett. **74**, 3209 (1995).